

This is a repository copy of *Examination of the Acoustic Spectrum in the Generalized Acoustic Analogy for Heated Flows - Temperature Coupling Effects vs Direct Enthalpy Flux Generated Noise*.

White Rose Research Online URL for this paper:

<https://eprints.whiterose.ac.uk/214068/>

Version: Accepted Version

Proceedings Paper:

Stirrat, Sarah, Koshuriyan, Zamir and Sescu, Adrian (2023) Examination of the Acoustic Spectrum in the Generalized Acoustic Analogy for Heated Flows - Temperature Coupling Effects vs Direct Enthalpy Flux Generated Noise. In: International Conference on Flow Dynamics. International Conference on Flow Dynamics, 06-08 Nov 2023 , JPN

Reuse

This article is distributed under the terms of the Creative Commons Attribution (CC BY) licence. This licence allows you to distribute, remix, tweak, and build upon the work, even commercially, as long as you credit the authors for the original work. More information and the full terms of the licence here:

<https://creativecommons.org/licenses/>

Takedown

If you consider content in White Rose Research Online to be in breach of UK law, please notify us by emailing eprints@whiterose.ac.uk including the URL of the record and the reason for the withdrawal request.

Examination of the Acoustic Spectrum in the Generalized Acoustic Analogy for Heated Flows - Temperature Coupling Effects vs Direct Enthalpy Flux Generated Noise

Sarah Stirrat¹, M.Z.A Koshuriyan², Adrian Sescu³

¹ Department of Mechanical & Aerospace Engineering, University of Strathclyde
75 Montrose St, Glasgow, G1 1XJ, United Kingdom

² Department of Mathematics, University of York,
James College, York, YO10 5DD, United Kingdom

³ Department of Aerospace Engineering, Mississippi State University,
501 Hardy Road, Starkville, MS 39762, USA

ABSTRACT

The generalized acoustic analogy remains one of the most robust jet noise prediction models for jets of arbitrary cross section. In 2011, Afsar, Goldstein & Fagan (AGF)[1] formulated a jet noise model which reduced the acoustic spectrum formula to one involving 11 independent components of the spectrum of the turbulence auto-covariance tensor. In this paper we calculate this spectral tensor using a validated in-house LES code to obtain the unsteady flow. We assess the difference between heated and cold inflow conditions at fixed $Ma = U_j/c_\infty$.

1. Introduction

Jet noise predictions using the generalized acoustic analogy (predecessors and variants) separate the problem of acoustic propagation and noise source modeling. This de-coupling of effects that fluid mechanically must be interrelated follows only when the turbulence structure (via its auto-covariance statistics) is assumed known. The sound radiated by known sources can then be calculated by determining the appropriate Green's function of the linearized Euler operator. In this paper we focus on low speed jets (acoustic Mach numbers less than 0.9) where non-parallel flow effects make little contribution to the low frequency spectral amplification. The Green's function is then the frequency domain solution to the Rayleigh equation. Using this within the acoustic analogy formula will allow predictions of sound to be made.

Our goal in this paper however is not simply the acoustic predictions (which have been done by numerous other authors). We, however, focus our attention on the spatial structure of the spectral tensor (which AGF [1] reduced to 11 components). The spectral tensor components are given in Table 1. These components are the space-time Fourier transforms of the physically measurable turbulence quantities. The latter is found by post-processing an unsteady flow data solution that we obtained using a previously validated in-house LES code. The calculations were performed at Mississippi State University. We have considered 4 round jet operating points for subsonic heated/isothermal flow conditions. The main aims of this work are:

1. Run LES to obtain unsteady data
2. Post-process the unsteady flow data to obtain the physical-space turbulence fourth order correlations.
3. Use item (2) to determine the spectral tensor components numerically

4. Include propagator and calculate acoustic spectrum

Item (3) in the list above is the novel feature of our work in this paper. The spectral tensor components appear in the AGF[1] acoustic spectrum formula as being the mathematical entities encapsulating the flow turbulence in the model. If they can be determined without having to obtain the physical space tensorial components in the acoustic spectrum formula (and if they are universal) it would make a significant reduction in complexity of the acoustic analogy approach. AGF's formulation was analyzed qualitatively. Our work assesses the numerical structure of their final acoustic spectrum formula using LES database.

2. LES Validation

The LES was performed using an in-house implicit LES solver which uses the 2nd order Adams-Bashforth time marching method. The mesh was composed of 13,244,832 cells and the computational time was roughly one week. Fig. 1 shows the mesh at the nozzle. Fig. 2 compares the LES results with several experimental [2, 3, 4, 5] and LES data [6, 7] from the literature for a cold jet at $Ma = 0.9$, showing good agreement. Similarly, Fig. 3 compares a hot jet also at $Ma = 0.9$ with experiment.

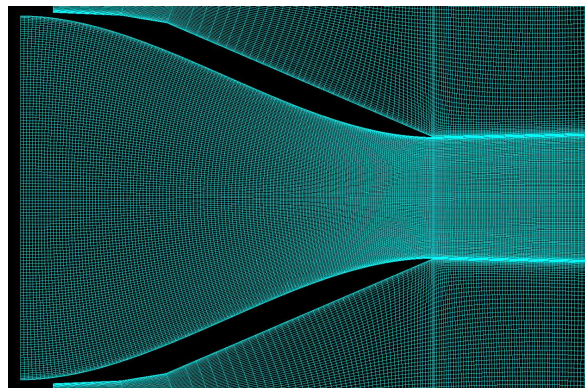
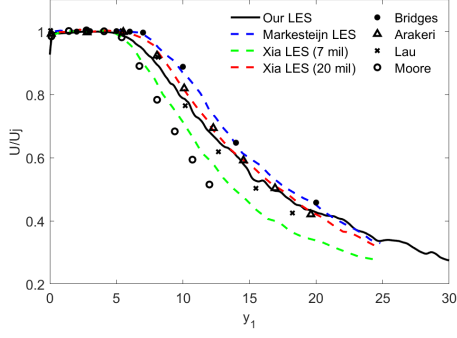
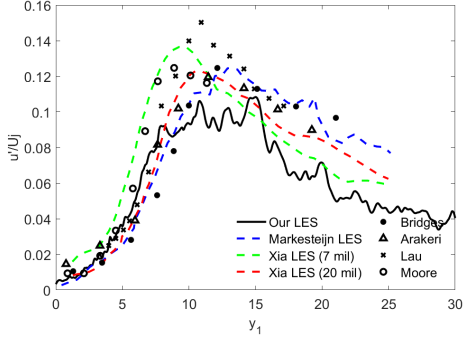


Fig. 1 LES mesh at nozzle.

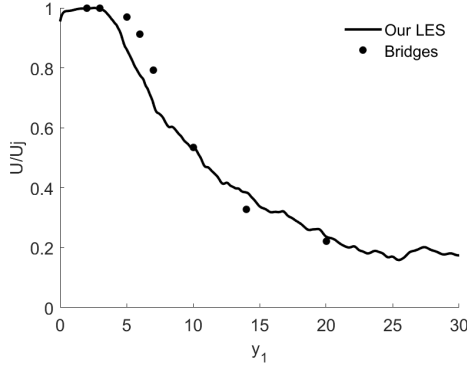


(a)

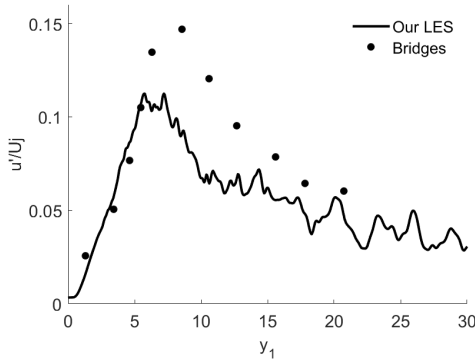


(b)

Fig. 2 $Ma = 0.9, TR = 0.87$: Validation of LES (a) meanflow U (b) turbulence intensity u' .



(a)



(b)

Fig. 3 $Ma = 0.9, TR = 2.7$: Validation of LES (a) meanflow U (b) turbulence intensity u' .

3. AGF Formula

AGF [1] showed that the acoustic spectrum can be written as a summation of the three basic sound production components. That is, sound generated by momentum flux (i.e. Reynolds stress only), enthalpy flux (temperature fluctuations) and coupling terms involving the interaction between these two. This formula is shown below in Eqn. 2.

$$I_\omega(\mathbf{x}|\mathbf{y}) = \sum_{n=1}^3 I_\omega^{[n]}(\mathbf{x}|\mathbf{y}) \quad (1)$$

where

$$I_\omega^{[1]} = G_{ij}(\mathbf{x}|\mathbf{y}; \omega) G_{kl}^*(\mathbf{x}|\mathbf{y}; \omega) \Phi_{ij,kl}^*(\mathbf{y}, \mathbf{k}, \omega) \quad (2a)$$

$$I_\omega^{[2]} = 2Re\Gamma_{4j}(\mathbf{x}|\mathbf{y}; \omega) G_{kl}^*(\mathbf{x}|\mathbf{y}; \omega) \Phi_{4j,kl}^*(\mathbf{y}, \mathbf{k}, \omega) \quad (2b)$$

$$I_\omega^{[3]} = \Gamma_{4j}(\mathbf{x}|\mathbf{y}; \omega) \Gamma_{4l}^*(\mathbf{x}|\mathbf{y}; \omega) \Phi_{4j,4l}^*(\mathbf{y}, \mathbf{k}, \omega) \quad (2c)$$

and G_{ij} is the propagator related to the vector Green's function of the adjoint linearized Euler equations given by Eq.(6) in [1].

Our concern in this paper, is the structure of the spectral function Φ which enters the acoustic spectrum by the following components in Table. 1 when an appropriate axisymmetric approximation is made.

Table 1 Spectral Tensor Components.

	Spectral Tensor Components	Independent Components
Momentum flux term	Φ_{ijkl}	$\Phi_{1111}, \Phi_{2222}, \Phi_{1212}, \Phi_{2323}, \Phi_{1122}, \Phi_{2211}$
Enthalpy flux/momentum flux coupling term	Φ_{4jkl}	$\Phi_{4111}, \Phi_{4122}, \Phi_{4221}$
Enthalpy flux term	Φ_{4j4l}	Φ_{4141}, Φ_{4242}

Φ is given by:

$$\Phi_{\nu j, \mu l}(\mathbf{y}, \mathbf{k}, \omega) = \int_{\eta} \mathcal{H}_{\nu j, \mu l}(\mathbf{y}, \eta, \omega) e^{-\mathbf{k} \cdot \eta} d\eta \quad (3)$$

where $\mathcal{H}_{\nu j, \mu l}$ is linearly related to the temporal Fourier transform of the measured Reynolds stress auto-covariance tensor.

We can then analyse the spatial structure of components in Table. 1 via the measured spectral tensor:

$$\Psi_{\nu j, \mu l}(\mathbf{y}; \mathbf{k}, \omega) = \int e^{ik_2 \eta_2 + ik_3 \eta_3} F_{\nu j, \mu l}(\mathbf{y}, \eta_2, \eta_3; k_1, \omega) d\eta_2 d\eta_3 \quad (4)$$

where $F_{\nu j, \mu l}$ represents the time and stream-wise numerical Fourier transform of the LES-extracted Reynolds stress auto-covariance. If we assume that $F_{\nu j, \mu l}$ depends on magnitude only (i.e. $F_{\nu j, \mu l}(\mathbf{y}, \eta_2, \eta_3, k_1) = F_{\nu j, \mu l}(\mathbf{y}, \eta_{\perp}, k_1)$), then the

measured spectral tensor can be reduced to a Hankel transform:

$$H_{\nu j, \mu l}(\mathbf{y}; k_1, k_{\perp}, \omega) = \int_0^{\infty} \eta_{\perp} F_{\nu j, \mu l}(\mathbf{y}; k_1, \eta_{\perp}, \omega) J_0(k_{\perp} \eta_{\perp}) d\eta_{\perp} \quad (5)$$

where J_0 is the Bessel function of the first kind of order 0. This approximation is consistent with assuming the jet turbulence is axisymmetric[1].

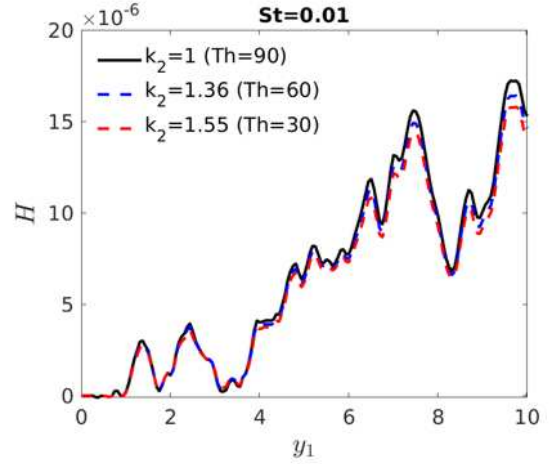
The wavenumbers k_1, k_{\perp} are only dependant on frequency and far field angle, θ , therefore the Hankel transform is only dependant on jet location, \mathbf{y} , St , and θ itself. In Fig. 4 we show the spatial structure of H_{1111} for a cold jet ($TR = 0.87$) at $Ma = 0.9$ along the shear layer $r = 0.5$. We can see that the Hankel transform decreases in magnitude as the St increases. The observation angle, $\theta = 90$ contributes greatest to the Hankel transform, however at small St the structure is uniform with θ , whereas at peak St and higher, as θ gets closer to the nozzle centerline (i.e. $\theta \rightarrow 0$), the Hankel transform decreases. In terms of spatial structure, for small St , the Hankel transform increases as y_1 increases, whereas for high St the structure is highly oscillatory across all y_1 .

Fig. 5 similarly shows the spatial structure of the Hankel transform for the hot jet ($TR = 2.7$) also at $Ma = 0.9$. Comparing this with the cold jet we can see that the overall trends remain similar. However, the magnitude of H-transform is smaller than that for the cold jet. Since the acoustic spectrum formulae in Eqs. (1) & (2), are proportional to the H-transform, the reduction in its magnitude will cause a direct reduction in the radiated sound.

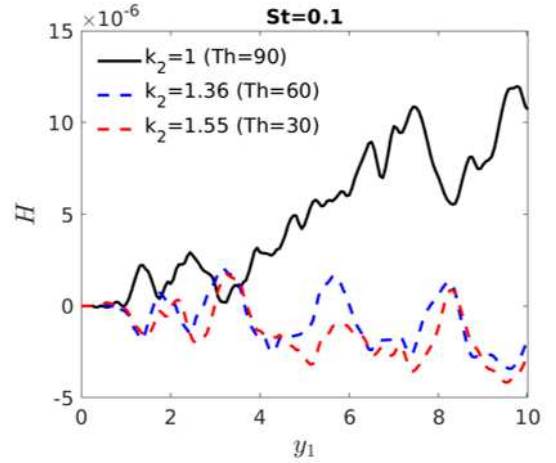
In the accompanying presentation we show how this data can be used for actual jet noise predictions.

References

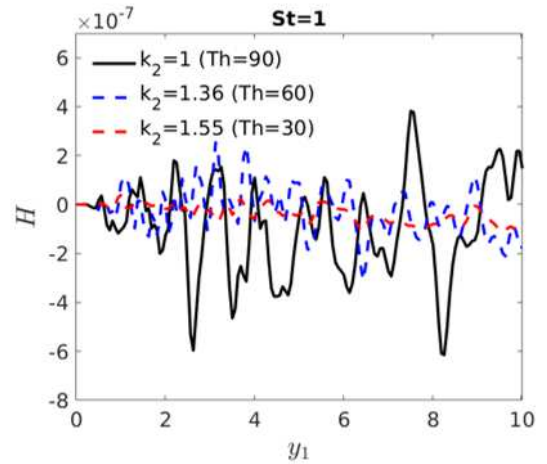
- [1] M.Z. Afsar, M.E. Goldstein, and A. Fagan, *AIAA J* 49, (2011), 2522–2532.
- [2] J. Bridges, M. Wernet, *NASA/TM* 2011-216807, (2011)
- [3] J.C. Lau, P.J. Morris, and M. Fisher, *J. Fluid Mech* 93 (1979), 1–27
- [4] V.H. Arakeri, A. Krothapalli, and A. Sidavaram, M.B. Alkislal, and L.M. Lourenco *J. Fluid Mech* 490, (2003), 75–98
- [5] C.J. Moore, *J. Fluid Mech* 80, (1977), 321–367
- [6] A.P. Markesteijn, S. Karabasov, *C.R. Mecanique* 346, (2018), 948–963
- [7] H. Xia, *Computers & Fluids* 110, (2015), 189–197



(a)

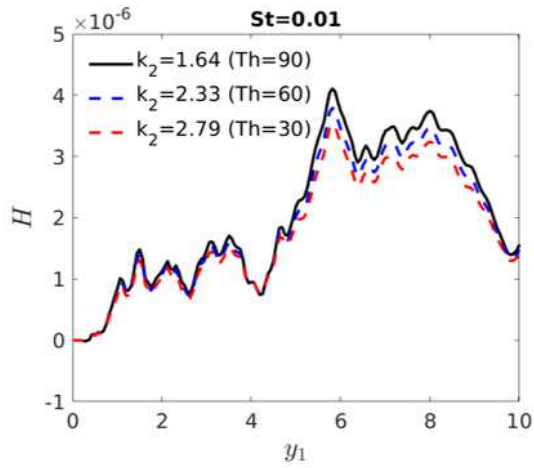


(b)

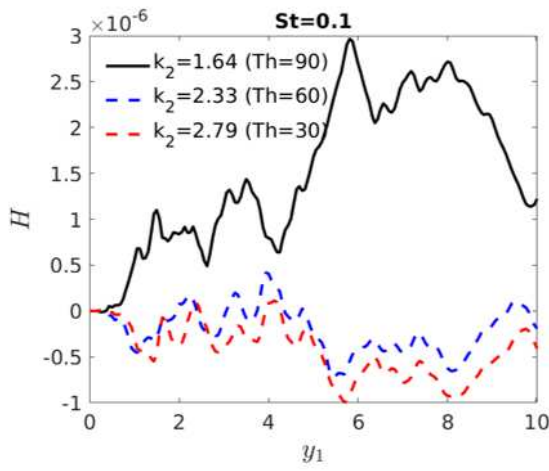


(c)

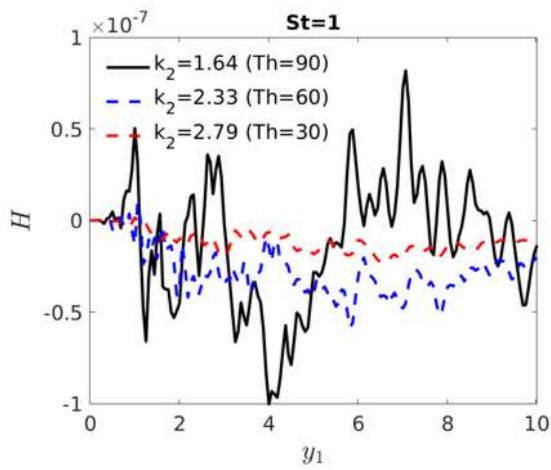
Fig. 4 $Ma = 0.9, TR = 0.87$: Spatial structure of Hankel transform at (a) $St = 0.01$ (b) $St = 0.1$ (c) $St = 1.0$.



(a)



(b)



(c)

Fig. 5 $Ma = 0.9, TR = 2.7$: Spatial structure of Hankel transform at (a) $St = 0.01$ (b) $St = 0.1$ (c) $St = 1.0$.